Under the influence of alcohol: The effect of ethanol and methanol on lipid bilayers

Michael Patra

Biophysics and Statistical Mechanics Group, Laboratory of Computational Engineering, Helsinki University of Technology, P. O. Box 9203, FIN–02015 HUT, Finland

Emppu Salonen, Emma Terama, and Ilpo Vattulainen

Laboratory of Physics and Helsinki Institute of Physics, Helsinki University of Technology, P. O. Box 1100, FIN–02015 HUT, Finland

Roland Faller and Bryan W. Lee

Department of Chemical Engineering and Materials Science, University of California-Davis, One Shields Ave, Davis, CA 95616, USA

Juha Holopainen

Department of Ophthalmology, University of Helsinki, Finland and Helsinki Biophysics & Biomembrane Group, Institute of Biomedicine, University of Helsinki, Finland

Mikko Karttunen

Biophysics and Statistical Mechanics Group, Laboratory of Computational Engineering, Helsinki University of Technology, P. O. Box 9203, FIN–02015 HUT, Finland

Extensive microscopic molecular dynamics simulations have been performed to study the effects of short-chain alcohols, methanol and ethanol, on two different fully hydrated lipid bilayer systems in the fluid phase at 323 K. It is found that ethanol has a stronger effect on the structural properties of the membranes. In particular, the bilayers become more fluid and permeable: Ethanol molecules are able to penetrate through the membrane in typical time scales of about 200 ns whereas for methanol that time scale is considerably longer, at least of the order of microseconds. We find good agreement with NMR and micropipette studies. We have also measured partitioning coefficients and the rate of crossing events for alcohols, i. e., typical time scale it takes for a molecule to cross the lipid bilayer and to move from one leaflet to the other. For structural properties, two-dimensional centre of mass radial-distribution functions indicate the possibility for quasi long-range order for ethanol–ethanol correlations in contrast to liquid-like behaviour for all other combinations.

I. INTRODUCTION

It is well known that even small changes in the composition of cell membranes can strongly affect the functioning of intrinsic membrane proteins, such as ion and water channels, which regulate the chemical and physical balance in cells (Cantor, 2003; Mazzeo et al., 1988). Such changes may occur due to the introduction of short-chain alcohols, or other anaesthetics, at membrane surfaces. Although anaesthetics are being used every single day in hospitals around the world, the molecular level mechanisms of general anaesthesia remain elusive, see e. g. (Cantor, 1997; Eckenhoff, 2001; Tang and Xu, 2002). The same applies to the effect of alcohols on biological systems. Klemm (1998) provides a good review of the topic.

Another aspect to the effect of alcohols appears in a more applied context. In the process of producing alcoholic beverages, wine in particular, yeasts like *saccharomyces cervisiae* have to sustain high ethanol concentrations without losing their viability. However, in about 10 % of all wine fermentations the industry encounters so-called stuck fermentations (Bisson and Block, 2002; da Silveira et al., 2003). There is no satisfactory understanding of this effect. Some models propose that an effect very similar to general anaesthesia is responsible for rendering the yeast cells dormant (Cramer et al., 2002). It has been suggested that high alcohol concentrations change the membrane structure and force transmembrane proteins into unfavourable conformations. In these conformations proteins cannot fulfil their functions and thus the yield drops dramatically.

In addition to the above aspects, there are other important issues as well. In particular, in cellular systems such as bacteria and yeast, the toxicity of ethanol has been suggested to be due to its interaction with membranes (da Silveira et al., 2003; Ly et al., 2002; Ly and Longo, 2004) and the consequent general effects such as changes in mechanical properties, permeability and diffusion. Changes in such generic membrane properties may affect the functions of proteins and binding sites due to changes in lateral pressure (Eckenhoff, 2001), or, if the membrane becomes more permeable, changes in the electrostatic potential may affect signalling. These effects are not to be mixed up with the toxicity due to metabolic products such as acetaldehyde from consump-

tion of ethanol – the cause of poisoning commonly known as hangover.

We concentrate on the effects of ethanol and methanol on structural properties of membranes. It is quite surprising that despite a vast number of clinical and biochemical studies, there has been very few computational investigations of the effect of short-chain alcohols, or other anaesthetics, on membranes. The only simulational studies of bilayers and ethanol are, to the authors' knowledge, the one by Feller et al. (2002) who used molecular dynamics simulations of ethanol and POPC (palmitoyloleoylphosphatidylcholine) lipid bilayers and NMR to study the molecular level interactions in these systems, and the article by Lee et al. (2004) discussing alcohol–membrane systems briefly. Direct comparison of our results with Feller et al. is not meaningful since their study was performed using a different ensemble close to the gel state at 283 K whereas here we are in the biologically relevant fluid phase at 323 K. For methanol–bilayer systems there exists to the authors' knowledge only one computational article (Bemporad et al., 2004).

For anaesthetics the situation is slightly better. Tang and Xu (2002) used molecular dynamics simulations to study molecular level mechanisms of general anaesthesia using halothane as a specific anaesthetic. They concluded that the global effects of anaesthetics, i. e., due to generic interaction mechanisms, are important and lead to modulations in the functions of channels and / or proteins. These conclusions are also supported by the fact that the same anaesthetics are effective for humans and a variety of animals. Similar conclusions for halothane interactions with bilayers have been pointed out by Koubi et al. (2001, 2000). The importance of generic effects has also been indicated in recent experimental studies of the effect of ethanol on *Oenococcus oeni* cells (da Silveira et al., 2003). Although the shortage of simulational studies may be due to the high computational demands of these systems, it is still surprising since computer simulations can provide detailed information about fundamental molecular level mechanisms.

In this article we study the effect of two short-chain alcohols, ethanol and methanol, on two different lipid membranes consisting of either pure DPPC (dipalmitoylphosphatidylcholine) or POPC. Methanol is a small solute having a single hydrophilic hydroxyl group whereas ethanol possesses an additional hydrophobic carboxyl group. DPPC and POPC share the same headgroup but one of the tails of POPC has a double bond and is two carbon atoms longer, whereas DPPC has only single bonds in its chains, see Fig. 1. We have studied these systems under fully hydrated conditions using microscopic molecular dynamics. 50 ns trajectories for each of the four combinations of lipid and alcohol allow us to gather high statistical accuracy.

Phospholipid bilayers can be considered as a first approximation to understand the behaviour of cell membranes under the influence of alcohol, and much information can be extracted from such systems. The simula-

tions show that ethanol is able to pass through the bilayer much more easily than methanol. This can be explained by the hydrophobic nature of the carbon "tail" of ethanol, making passing through the hydrophobic tail regions of lipid bilayers easier. In addition, ethanol molecules condense near the interface region between lipids and the surrounding water, i. e., there is a sharply increased density of ethanol near the interface region, while for methanol only a moderate increase of the density is seen near the interface region. These effects are very pronounced for DPPC bilayers, and only slightly weaker for POPC bilayers. This has far reaching implications for the basic properties of bilayers.

The rest of this article is organised as follows. In the next section we describe the model and the simulation details. Then, in Sec. III, we present the results from the simulations. Section IV contains a discussion and conclusions.

II. MODEL AND SIMULATION DETAILS

We have simulated lipid bilayer systems consisting of either 128 DPPC or 128 POPC molecules (i. e., 64 lipids in each leaflet). For the lipids we used a previously validated united atom model (Tieleman and Berendsen, 1996). The DPPC simulations are based on the final structure of a 100 ns run of a DPPC bilayer that is fully hydrated by 3655 water molecules. The configuration is available online[1]. The simulations by Patra et al. (2004) were run using the same parameters as here (details below), and the 100 ns run used in this study is a continuation of a 50 ns study (Falck et al., 2004; Patra et al., 2004). For the POPC simulations, such an initial structure had to be generated first. We started with a fully hydrated POPC bilayer (Tieleman et al., 1999) and simulated it for 10 ns. The final structure of that simulation run was used as a starting point for the POPC simulations reported here.

In order to add the alcohol molecules, the simulation box was first extended in z-direction such that an empty volume was created. A total of 90 ethanol (methanol) molecules were randomly inserted in the empty volume, and the remaining space was filled with water. The total number of water molecules then amounted to 8958 for the DPPC systems and 8948 for the POPC systems, or, in other words, 1 mol% alcohol on a lipid free basis. The small difference between DPPC and POPC systems is due to the different lateral extensions of the bilayers.

The force field parameters for bonded and non-bonded interaction were taken from Berger et al. (1997), available online[2]. Partial charges were taken from Tieleman and Berendsen (1996), available online for both DPPC [3] and POPC [4]. As is seen in the chemical structures in Fig. 1, DPPC and POPC are identical up to a single pair of CH-groups, connected by a double bond

---

[1] http://www.softsimu.org/downloads.shtml
[2] http://moose.bio.ucalgary.ca/Downloads/files/lipid.itp
[3] http://moose.bio.ucalgary.ca/Downloads/files/dppc.itp
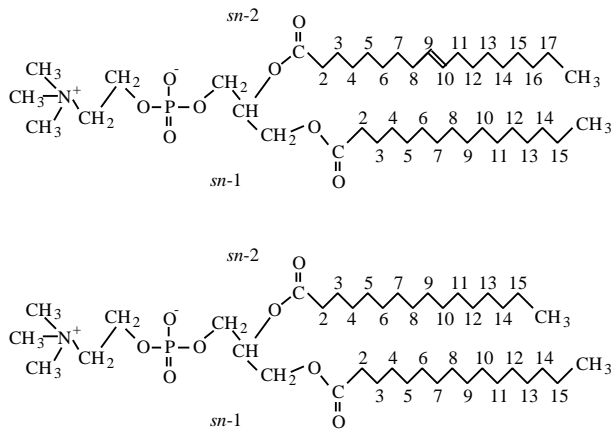[4] http://moose.bio.ucalgary.ca/Downloads/files/popc.itp

FIG. 1 Structures of POPC (top) and DPPC (bottom). They are identical with the exception of the $sn-2$ chain which is two carbons longer and contains one double bond for POPC.

instead of a single bond in the $sn-2$ chain of POPC, and the two additional CH_2 groups at the end of that chain. This similarity is reflected in the force fields, which are identical up to the modelling of the four affected atoms. Ethanol and methanol were modelled using the Gromacs force field parameters (Lindahl et al., 2001) which are identical with the exception of the added CH_2 group for ethanol. Thus, differences observed between the two lipids or the two alcohols do not originate from differences in their respective force field parameterisations but are due to the physics and / or chemistry of those components. For water the Simple Point Charge (SPC) model (Berendsen et al., 1981) was used.

The simulations were performed with the Gromacs package (Lindahl et al., 2001). The lipids, water molecules and alcohols were separately coupled to a heat bath at temperature $T = 323$ K using the Berendsen thermostat (Berendsen et al., 1984) with a coupling time constant of 0.1 ps. All the bond lengths were constrained to their equilibrium values by the Lincs algorithm (Hess et al., 1997). Pressure was controlled using the Berendsen barostat (Berendsen et al., 1984) with a time constant of 1 ps. The pressure coupling was used semi-isotropically such that height of the box (z direction) and the cross sectional area (xy-plane) were allowed to vary independently of each other. Lennard-Jones interactions were cut off at a distance of 1.0 nm and the time step was set to 2 fs. Long-range electrostatics were updated every 10-th time step [the twin-range scheme (Kessel et al., 2004; Patra et al., 2003) was used], and handled by the particle-mesh Ewald (PME) algorithm (Essman et al., 1995). For DPPC bilayers it has been shown that replacing PME by the computationally cheaper cut-off scheme leads to pronounced artifacts (Patra et al., 2003, 2004).

The systems were simulated for a total of 50 ns each. After 20 ns, the samples had equilibrated, and the remaining 30 ns were used for data collection. Equilibration was determined by monitoring the area per lipid as described in the next section. For completeness, we also present results for pure DPPC and POPC bilayers. In particular the latter ones are important since many of the results have so far only been published based on simulations using a cutoff for handling electrostatics. In addition to the above systems, we also performed a control simulation with a dehydrated system containing only

10 water molecules per lipid. This was done in order to see if dehydration has a direct effect on the properties but no significant effects were found.

The simulations took a total of 16 000 CPU hours using an IBM eServer Cluster 1600 (Power4 processors).

III. SIMULATION RESULTS

Before presenting a systematic summary of our results, we give a quick overview of the basic properties of these systems. Alcohol molecules have a tendency to collect in or near the bilayer (Sec. III.B). This tendency is stronger for ethanol than for methanol as confirmed by a partition analysis (Sec. III.I). Ethanol is able to form hydrogen bonds with the lipids in the bilayer (Sec. III.D), and these hydrogen bonds reduce the order parameter of the lipid hydrocarbon tails. The combination of all this results in an easy penetration of ethanol through the bilayer. In contrast, no hydrogen bonds or penetration was observed for methanol.

In this paper we use the following colour code for all figures. Curves for systems containing ethanol are drawn in red, curves for methanol in green and pure lipid systems without alcohol in blue.

A. System dimensions

The area per lipid is one of the most important quantities characterising lipid bilayer systems and it can also be used to monitor equilibration during a simulation run. The time evolutions of the area per lipid in the systems studied here are shown in Fig. 2. The average areas per lipid, $\langle A \rangle$, obtained in our simulations are listed in Table I.

For a pure DPPC bilayer we obtain $\langle A_{DPPC} \rangle = 0.655$ nm^2 agreeing well with previous simulations and experiments, see Ref. (Patra et al., 2003) and references therein. For pure POPC we obtain $\langle A_{POPC} \rangle = 0.677$ nm^2 in agreement with previous computational
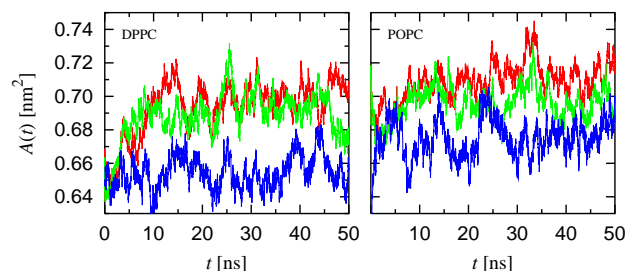

FIG. 2 Temporal behaviour of the area per lipid $A(t)$ for a DPPC bilayer (left) and a POPC bilayer (right). The colour of the line marks whether the lipid bilayer has been simulated in the presence of ethanol (red), of methanol (green), or of no alcohol (blue). This is our standard colour code employed throughout this paper.

System	Average area per lipid
DPPC (pure)	(0.655 ± 0.002) nm^2
DPPC + ethanol	(0.699 ± 0.002) nm^2
DPPC + methanol	(0.693 ± 0.004) nm^2
POPC (pure)	(0.677 ± 0.003) nm^2
POPC + ethanol	(0.699 ± 0.003) nm^2
POPC + methanol	(0.693 ± 0.003) nm^2

TABLE I Average area per lipid for all systems studied in this work. A weak effect of the alcohols is visible. The error estimates have been computed from block averaging and extrapolating to large block sizes.

studies (Chiu et al., 1999; Pasenkiewicz-Gierula et al., 2003) and slightly larger than the results from x-ray diffraction studies (Pabst et al., 2000a,b). For POPC, the difference to x-ray diffraction results $\langle A_{\mathrm{POPC}} \rangle \approx 0.61$ nm^2 may be due to differences in trans-gauche conformational changes.

As seen from Table I, the presence of alcohol has a small but non-vanishing effect on the area per lipid. The number of water molecules per lipid molecule plays only a minor role as was verified by an additional simulation of DPPC with ethanol and a reduced amount of water. Interestingly, ethanol and methanol have almost the same effect on the area per lipid.

While the definition of the area per lipid is straightforward, the same is not true for the volume occupied by a lipid. The precise definition of the volume V (or the thickness d) of a membrane is non-trivial as discussed at length by Armen et al. (1998). Here, we chose an operational definition based on local mass density. Other definitions, e. g., employing the electron density, are equally possible.

Below, we give the two definitions we used to compute the thickness. If ρ_{lipid}, ρ_{water} and ρ_{alcohol} are the mass densities of the three components, the effective thickness

of a single leaflet can be defined by

$$d_1 = \frac{1}{2} \int \frac{\rho_{\mathrm{lipid}}}{\rho_{\mathrm{lipid}} + \rho_{\mathrm{water}} + \rho_{\mathrm{alcohol}}} \mathrm{d}z \, , \qquad (1\mathrm{a})$$

$$d_2 = \frac{1}{2} \int \frac{\rho_{\mathrm{lipid}}}{\rho_{\mathrm{lipid}} + \rho_{\mathrm{water}}} \mathrm{d}z \, . \qquad (1\mathrm{b})$$

These two definitions differ in their treatment of the alcohol volume fraction and give the same thickness for pure lipid bilayers. After defining the thickness, the volume is simply $V = d\langle A \rangle$ with $\langle A \rangle$ being the average area per lipid. The results using both of the above definitions are summarised in Table II.

The thicknesses we obtained for pure POPC agree very well with recent x-ray diffraction studies of Vogel et al. (2000) and computer simulation studies of Gullingsrud and Schulten (2004) who obtained 3.9 nm and 3.92 nm, respectively, for the total bilayer thickness $2\,d$. For DPPC the thickness and volume are a few percent larger than the experimental results (Nagle and Tristram-Nagle, 2000). Using the electron density to define the thickness would have led to similar results, see Sec. III.C.

A comparison of Tables I and II shows that the addition of ethanol or methanol to a bilayer expands its surface slightly while the thickness decreases such that the volume per lipid does not change significantly. This is as assumed since the main effect of the addition of alcohol is a reduction of the surface tension of the water phase. This is in agreement with observations from a DPPC–halothane system (Tu et al., 1998). We will return to this issue in Sec. IV.

To complement the average area per lipid $\langle A \rangle$ measurements, we have also computed the area probability distribution $P(A)$ by Voronoi tessellation. By definition, Voronoi tessellation measures the area that is closer to a given molecule than to any other one. The Voronoi approach does not uniquely specify which point should be used to represent the entire molecule. We used the centre-of-mass position of each lipid, projected onto the xy-plane. Other choices are also possible, such as the position of the $sn-3$ carbon which gives a better indication of the backbone of the lipid whereas the centre-of-mass describes the entire lipid.

System	d_1 [nm]	V_1 [nm^3]	d_2 [nm]	V_2 [nm^3]
DPPC (pure)	2.02 ± 0.05	1.32 ± 0.03	2.02 ± 0.05	1.32 ± 0.03
with ethanol	1.84 ± 0.02	1.28 ± 0.02	1.90 ± 0.02	1.33 ± 0.02
with methanol	1.93 ± 0.06	1.34 ± 0.04	1.95 ± 0.06	1.35 ± 0.04
POPC (pure)	1.96 ± 0.04	1.33 ± 0.03	1.96 ± 0.04	1.33 ± 0.03
with ethanol	1.87 ± 0.02	1.31 ± 0.02	1.93 ± 0.03	1.35 ± 0.02
with methanol	1.94 ± 0.02	1.35 ± 0.01	1.96 ± 0.02	1.36 ± 0.01

TABLE II The thickness d of a leaflet (the bilayer thickness is twice that value) and the corresponding volume per lipid using the two definitions given in Eq. (1). The error estimate for d has been computed by cutting the analysis part of the trajectory in two parts and by applying Eq. (1) separately to both of them.
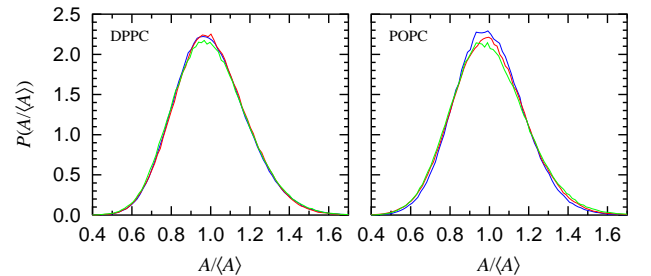

FIG. 3 Distribution of the individual areas of the lipids as determined by two-dimensional Voronoi tessellation for DPPC (left) and POPC (right).
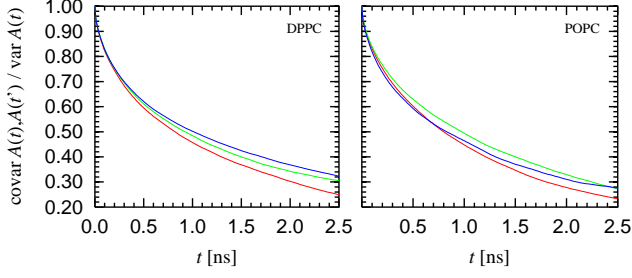
FIG. 4 Autocorrelation function for the individual areas of the lipids as determined by two-dimensional Voronoi tessellation for DPPC (left) and POPC (right).

FIG. 6 Mass density profiles across the bilayer for DPPC (left) and POPC (right). The density of the alcohol has been scaled by a factor of 10, and the colour code is the same as above.

The resulting distributions $P(A)$ are shown in Fig. 3. The mean of that distribution is, by construction, identical to the average area per lipid as shown in Table I, and thus does not contain any additional information. For this reason, not the plain distribution $P(A)$ but rather the re-scaled distribution $P(A/\langle A\rangle)$ is shown in Fig. 3. Plotting the result in this way shows that alcohol does not influence the Voronoi distribution in any way that would not be captured already by the average area per lipid.

It is also possible to compute the autocorrelation time of the Voronoi areas. This time gives an indication of how quickly the geometry of the bilayer changes locally whereas the fluctuations in the size of the simulation box seen in Fig. 2 are related to global changes of the geometry. The results are shown in Fig. 4. The faster decay for the systems with ethanol suggests that the bilayer might become more fluid but care should be taken in drawing conclusions as the differences between the curves are rather small.

Next, we perform similar Voronoi tessellation for the alcohol molecules inside the bilayer interface region. The precise definition of that region turned out not to be critical, and we included all alcohol molecules within the range 0.7 nm $< z <$ 1.7 nm from the centre of the bilayer. (Our choice for this range is motivated by the results to be discussed later in Sec. III.B.) The variable number of molecules forbids a proper calculation of the

correlation time for the areas assigned to each alcohol, though, and thus we present only the distribution $P(A)$ in Fig. 5. Since there are fewer methanol molecules close to the bilayer than there are ethanols (see Fig. 6), the average area per methanol is larger than the average area per ethanol.

B. Mass density

The mass density profiles across the bilayer are shown in Fig. 6. For each analysed simulation frame, the system was first translated such that the centre of the bilayer was located at $z = 0$. Particles with $z < 0$ were mirrored to $z > 0$ to reduce statistical error. The masses of the hydrogen atoms were accounted for in the calculation. Due to the low density of alcohol, its curve is scaled by a factor of 10 in the figure.

Additional information can be gained by considering separately the two charged groups in the lipid headgroups, namely the phosphate (P) and the choline (N) group (cf. Fig. 1). In addition to this, the oxygen atom of the alcohols is included in Fig. 7. We could not find a direct comparison for the mass density but the observations from the computer simulations of Feller et al. (2002) are consistent with our results for the mass density. Figure 7 shows that the alcohol molecules have a strong
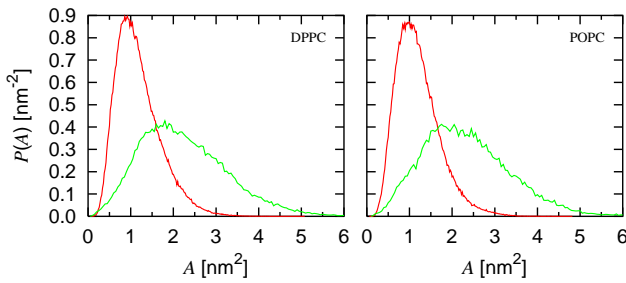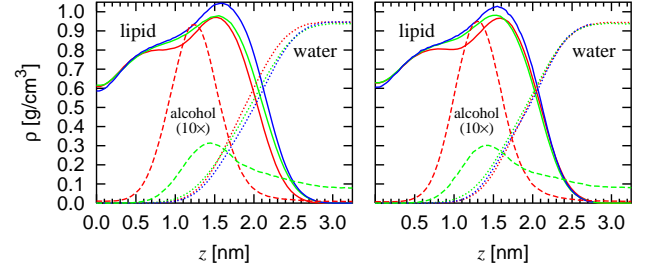

FIG. 5 Distribution of the Voronoi areas of the alcohols with DPPC (left) and POPC (right). Only alcohol molecules located close to the bilayer interface are included in the analysis.
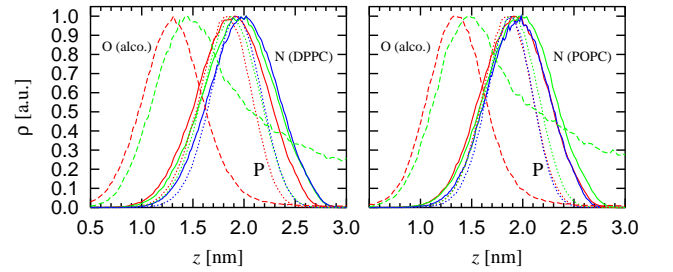

FIG. 7 Mass density profiles across the bilayer. The densities given are the O(xygen) of alcohol as well as N(itrogen) and P(hosphorus) of the lipid, and scaled to give a maximum of unity. Left for DPPC, right for POPC.
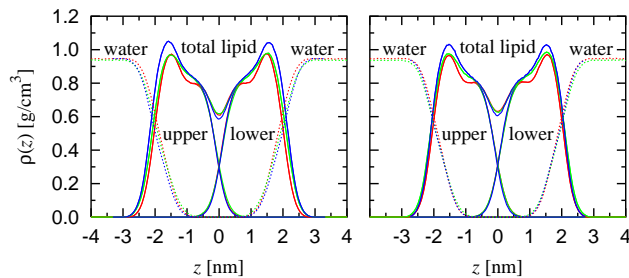
FIG. 8 Density profile across the whole bilayer. The lipid component is divided into the contributions from the two separate leaflets, providing a measure of interdigitation. The alcohol component has been suppressed in the figure. Left for DPPC, right for POPC.

FIG. 9 Electron density profiles in the studied systems with DPPC (left) and POPC (right).

tendency to accumulate below the bilayer–water interface layer (approximately given by the location of the phosphate and choline groups), and that this tendency is stronger for ethanol than for methanol. We will return to this issue in the partitioning analysis in Sec. III.I and the membrane penetration analysis in Sec. III.J.

The density of the lipid is decreased near the centre of the bilayer. This phenomenon is known as lipid trough and means that the two leaflets are repelling each other. Still, the tails of the lipids from one leaflet are able to penetrate into the other leaflet; this is known as interdigitation (Löbbcke and Cevc, 1995). To analyse this, in Fig. 8 we plot the density throughout the whole bilayer, i. e., the positions of all atoms are not folded into a single leaflet. We show separately the density of the lipids belonging to the upper and the lower leaflet of the bilayer. It is easily seen that the tails of the lipids can penetrate up to 0.5 nm into the other leaflet, and the degree of interdigitation is largely independent of the presence of alcohol.

C. Electron density

Electron densities provide information about the structure of bilayers along the normal to the bilayer plane similar to the mass densities. Experimentally, x-ray diffraction provides a means to access this quantity, the measurements yielding information of the total electron density profile.

Figure 9 shows the total electron densities in different cases. For the pure lipid bilayers, the curves show the typical behaviour, namely a maximum associated with the electron dense areas in the headgroup, i. e., the phosphate groups, and the minimum at the bilayer centre – the so-called methyl trough (Nagle and Tristram-Nagle, 2000). Experimentally, an electron density profile contains different information than a mass density profile since the chemical composition at depth z is not known directly. (For computer simulations this problem does not exist.)
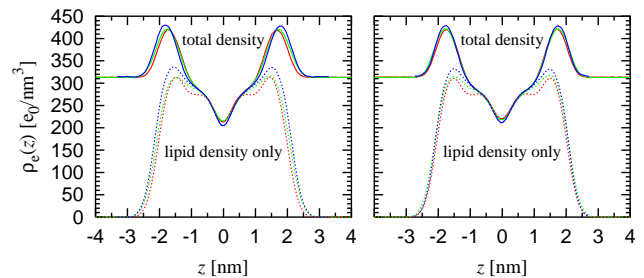
For the pure systems our results agree well with ex-

periments (Nagle et al., 1996). The only x-ray diffraction study in a related system containing ethanol or methanol that we are aware of is that of Adachi (2000). Unfortunately a direct comparison is not meaningful since that study was done in the gel phase using multilamellar vesicles as compared to the fluid-like phase and planar bilayer system studied here.

D. Hydrogen bonding of alcohol to lipids

As was shown in Sec. III.B, the alcohol molecules have a tendency to be located inside the bilayer, and this tendency is stronger for ethanol than for methanol. The alcohol molecules are not located directly at the water–membrane interface but rather further inside the bilayer. For the simulations with ethanol, a direct visual inspection of the atom positions shows that ethanol molecules are located close to the ester oxygens of the lipids, see Fig. 10.

This visual conclusion is confirmed by a hydrogen bonding analysis. In such an analysis, possible donors and acceptors are identified by their chemical properties, and a hydrogen bond is then assumed to exist whenever two such atoms and an additional hydrogen atom fulfil certain geometric conditions. (The distance between a hydrogen and an acceptor has to be smaller than 0.25 nm, and the angle between acceptor, hydrogen and donor has to be smaller than 60 degrees.)

The hydrogen bonding analysis shows that the majority of the ethanols are involved in hydrogen bonds with lipids whereas not a single hydrogen bond between a

	DPPC	POPC
bound ethanols	72.9	71.6
bound lipids	59.7	59.2
hydrogen bonds	74.1	72.8
lifetime [ns]	1.20	1.15

TABLE III Results of the hydrogen bonding analysis for the DPPC and POPC bilayers with ethanol. (The systems consist of 128 lipid molecules and 90 alcohol molecules.) No hydrogen bonds between methanol and lipids were found.
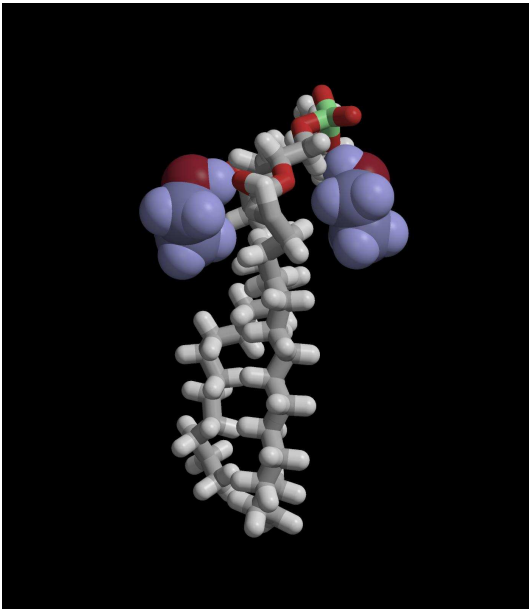
FIG. 10 A DPPC molecule together with two ethanol molecules. The ethanols are located close to the ester oxygen. The DPPC molecule is drawn as rods whereas the ethanols are drawn in a spacefilling representation. To aid the eye, the ethanols are coloured blue-ish.

methanol and a lipid molecule was found in our simulations. The results are summarised in Table III. Many lipids are involved in more than one hydrogen bond which comes as no surprise since they possess an ester oxygen in each of their two chains. Comparison with the lifetime data for ethanol in Table III with NMR experiments (Holte and Gawrisch, 1997) shows excellent agreement. In their experiments Holte and Gawrisch reported the lifetimes to be around 1 ns while we obtained 1.20 ns for the ethanol lipid hydrogen bonds. We are not aware of any such experiments for methanol.

The number of alcohol molecules involved in hydrogen bonds is best compared against the total number of alcohol molecules located inside the bilayer. The latter number is relatively ill-defined but from Fig. 6 one can easily compute that for ethanol-containing systems only of the order of 10 ethanol molecules out of the approximately 70 inside the bilayer are not involved in hydrogen bonds. For comparison, in the methanol systems there are of the order of 20 methanol molecules inside the bilayer and none of them is involved in hydrogen bonds (but cf. Sec. III.J). These numbers show that there indeed is a significant difference between ethanol and methanol.

Hydrogen bonding analysis offers a well-defined criterion to decide whether a given lipid is interacting strongly with an alcohol molecule or not. This will be used in the following sections to study separately the two lipid populations, lipids bound to an alcohol and lipids not bound to an alcohol.

E. Radial-distribution functions

In addition to the mass density profiles, valuable information may be gained from radial-distribution functions (RDFs). The radial-distribution functions $g(r)$ give the probability of finding two particles at a mutual distance r once geometric and density factors have been scaled out.

Figure 11 shows the RDFs between the oxygen of the alcohol and different charged groups inside the lipid. Some of these groups were depicted already in the mass density profile in Fig. 7 but whereas there only the vertical distance between particles was considered, the RDF considers the real three-dimensional distance between them.

While the mass density profile showed that on the average ethanol molecules prefer to reside 0.5 nm below the lipid headgroups, the RDF shows that the three-dimensional preferred distance is only 0.38 nm. This is no contradiction but is easily understood by the observation (cf. Fig. 17 a bit further down) that lipid molecules without an attached ethanol molecule are sticking out of the bilayer more than those with an attached ethanol. This is captured only by the RDFs but not by the mass density profile.

The radial-distribution functions for the different systems look quite similar – with one exception: The RDF between the alcohol and the ester group is peaked at a much smaller distance for ethanol than it is for methanol. This is in agreement with the results of the hydrogen bonding analysis.

By studying the mutual RDFs of the choline and / or phosphate groups, it is possible to detect phase transitions of the bilayer. Within error margins, these RDFs are not dependent on the presence of alcohol, and for space reasons we do not show them here as they are identical to the RDFs published previously (Patra et al., 2004).

We have also studied two-dimensional radial-distribution functions of entire molecules, i.e., the molecules' centres-of-masses were projected onto the
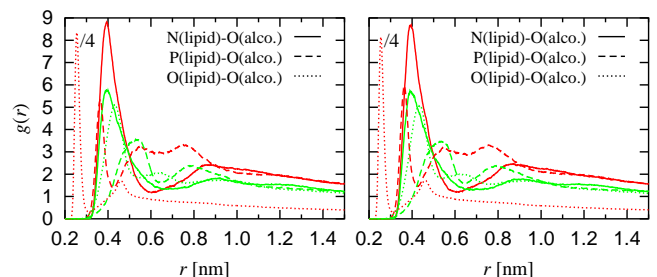

FIG. 11 Radial-distribution function between the oxygen of alcohol, on the one hand, and the phosphorus and the nitrogen atoms in the headgroup as well as the ester oxygens in the lipid tail, on the other hand. The oxygen–oxygen curve has been scaled by a factor of 1/4, i.e., in reality the RDF peaks at a value four times as large as displayed in the figure.
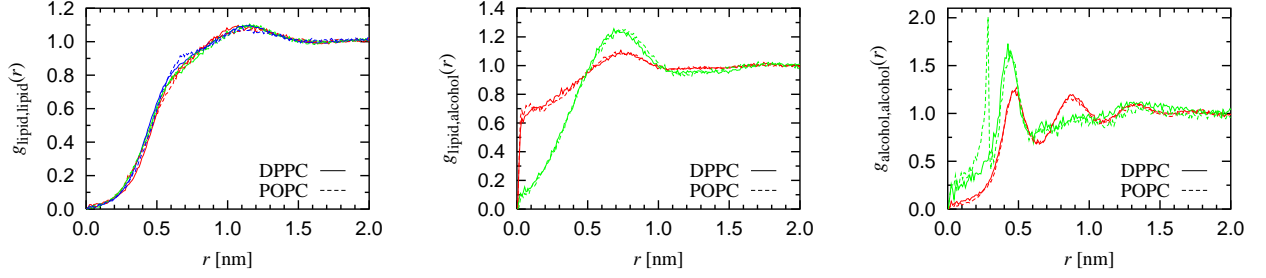
FIG. 12 Two-dimensional radial-distribution functions of the centre-of-mass positions for lipid–lipid (left), lipid–alcohol (centre) and alcohol–alcohol (right).

xy-plane and radial-distribution functions were then computed. The results are shown in Fig. 12. The mutual radial-distribution functions of the lipids exhibit a very soft core as lipids are able to wrap around each other. No dependence on lipid type or presence of alcohol was observed.

The RDF between alcohol and lipid is qualitatively different for ethanol and methanol. For an ethanol, there is a large probability for it to be at the same x-y position as the (centre-of-mass of the) lipid. This reflects the hydrogen bonding of ethanol close to the centre of the lipid. This bonding is absent for methanol, and consequently then $g(r) \to 0$ for $r \to 0$. No significant dependence on the kind of lipid is observed.

The alcohol–alcohol radial-distribution functions have a very different character: For methanol with DPPC, the first peak is very distinct but the correlations decay soon after. For methanol with POPC an additional peak is observed. (This is the only curve with a significant difference between DPPC and POPC. We cannot offer a convincing explanation for this.) For ethanol, the behaviour shows almost quasi long-range order. The reason for this ordering is not clear and further experiments would be needed to study this in detail.

F. Order parameters

Ordering of the lipid acyl chains is typically characterised using the order parameter tensor

$$S_{\alpha\beta} = \frac{1}{2} \left\langle 3\cos\theta_\alpha \, \cos\theta_\beta - \delta_{\alpha\beta} \right\rangle , \qquad (2)$$

where $\alpha, \beta = x, y, z$, and θ_α is the angle between the αth molecular axis and the bilayer normal (z-axis). The order parameter is then computed separately for all carbons along the acyl chain. Since lipid bilayer systems possess symmetry with respect to rotations around the z-axis, the relevant order parameter is the diagonal element S_{zz}. To relate S_{zz} to the experimentally relevant deuterium order parameter

$$S_{\text{CD}} = \frac{2}{3}S_{xx} + \frac{1}{3}S_{yy} , \qquad (3)$$

we use the symmetry and write $S_{xx} = S_{yy}$, and $S_{xx} + S_{yy} + S_{zz} = 0$. Using these relations we have $S_{\text{CD}} = -S_{zz}/2$. To allow comparison with experimental data, we present our results in terms of $|S_{\text{CD}}|$.

Since our simulations employ a united atom model, no explicit information about the hydrogen positions is available and they must be reconstructed assuming a perfect tetrahedral arrangement. The results are shown in
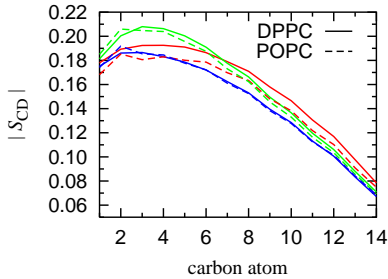

FIG. 13 Deuterium order parameters, computed from Eq. (3), for DPPC (solid line) and POPC (dashed line). For DPPC, the average over the two tail chains is displayed while for POPC only the saturated $sn-1$ chain is shown. For numbering of carbon atoms, refer to Fig. 1.
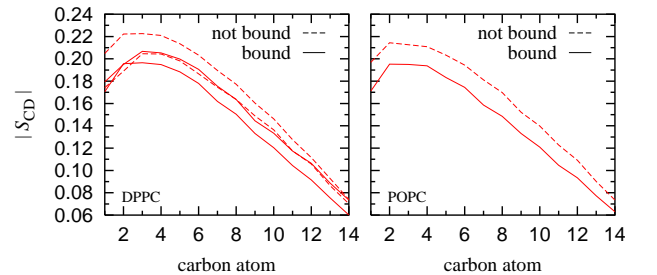

FIG. 14 Order parameter of DPPC (left) and POPC (right) in the presence of ethanol. For DPPC, both the $sn-1$ and $sn-2$ chains are shown whereas for POPC only the $sn-1$ chain is depicted. The order parameter has been computed separately for lipids that are bound to at least one alcohol molecule (solid lines), and for lipids that are not bound to any alcohol (dashed lines).
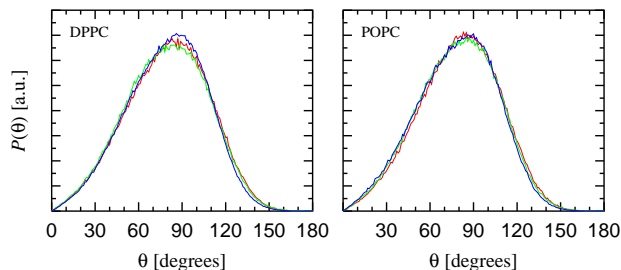
FIG. 15 Distribution of the angle θ between the $P-N$ vector and the bilayer normal for DPPC (left) and POPC (right).

Fig. 13. Reconstruction of the hydrogen positions means that for the outermost carbon atoms of the tail no order parameter can be constructed. This also includes positions where a sequence of carbon atoms connected by single bonds ends in a carbon atom having a double bond. It is not a problem to compute the order parameter for a chain of atoms connected by double bonds, there just is a problem connecting such a chain to a chain of atoms connected by single bonds. For this reason we show the order parameter for both chains of DPPC but for POPC we restrict ourselves to the saturated $sn-1$ chain, see Fig. 1.

The results for the order parameter for all the cases are shown in Fig. 13. We find that methanol increases ordering of the lipid acyl chains close to the glycerol group, while the effect of ethanol is strongest below the glycerol group, around the centre of the hydrocarbon tails. These results are fully consistent with the mass density profiles in Fig. 6.

As discussed in the introduction, there is, to our knowledge, only one other, related membrane–alcohol simulation study (Feller et al., 2002). In that the temperature was 40 degrees lower. Although direct comparison is not possible, the order parameters in that study and ours are in qualitative agreement. It is noticeable that the effect of alcohols on the average order parameter is small – this is consistent with the fact that the volume occupied by a lipid changes only slightly.
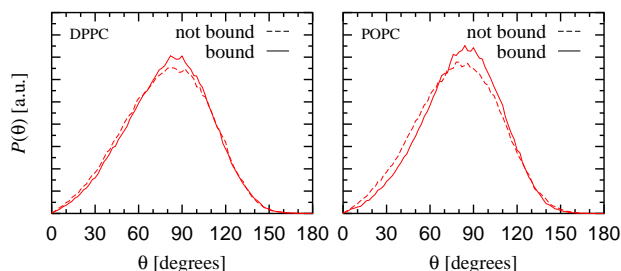

FIG. 16 Distribution of the angle between the $P-N$ vector and the bilayer normal for DPPC (left) and POPC (right) in the presence of ethanol. The distribution is separated into lipids that are hydrogen bonded respectively not hydrogen bonded to an ethanol molecule.
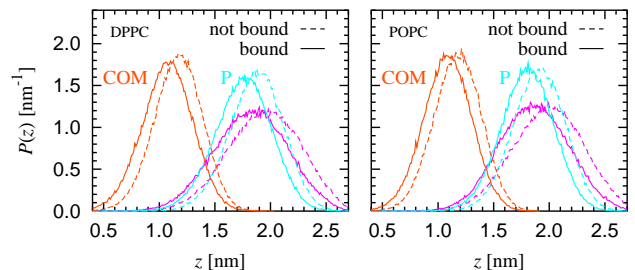

FIG. 17 Distribution of the position of the phosphate group (P), the choline group (N) and the centre-of-mass of the entire lipid (COM), left for DPPC, right for POPC. Results are shown as solid (dashed) lines for lipid molecules bound (unbound) to an ethanol molecule. Please note that in this figure the colours do not mark the kind of alcohol present.

Additional insight can be gained by combining the order parameters with the hydrogen bonding analysis from Sec. III.D. This combination allows the computation of the order parameter depending on whether the lipid forms a hydrogen bond with an alcohol molecule or not. The result in Fig. 14 shows that binding of ethanol slightly decreases the order of the tails.

In addition to the deuterium order parameter for the acyl chains, it is possible to study the ordering of headgroups in a similar fashion. To do that, we have chosen the angle of the $P-N$ vector with respect to the bilayer interface plane and have computed its distribution. The result is shown in Fig. 15. The $P-N$ vector has a significantly higher tendency of being in the bilayer plane ($\theta = 90°$) than of sticking out of it. The computed distribution is only slightly dependent on the presence of alcohol.

Again, we can obtain additional information for the ethanol systems if the angular distribution is separated into the distributions of lipids that are hydrogen bonded to an alcohol, and those that are not. The result is shown in Fig. 16. For DPPC the angular distribution is not influenced at all by hydrogen bonding whereas for POPC the influence is small.

To better explain the results presented in this section, we return to the mass density profiles. We analysed the positions of the phosphate and the choline groups in the heads of the lipids as well as the lipids' centre-of-mass positions, separated into lipids that are hydrogen bonded or not hydrogen bonded to an ethanol. The data in Fig. 17 shows that lipid molecules are shifted towards the centre of the bilayer by approximately 0.2 nm if they are bonded to an ethanol molecule. This is in agreement with the reduced order parameter as that is normally associated with a thinner bilayer. The vertical distance between the choline and the phosphate group remains unchanged, in agreement with the distribution of the $P-N$ angle.
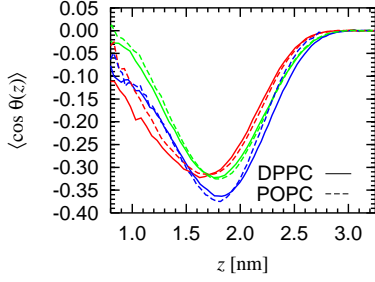
FIG. 18 Water orientation, as described by the mean cosine of the angle of the water dipole moment with respect to the bilayer normal.

FIG. 19 Electrostatic potential through the bilayer for DPPC (top) and POPC (bottom).

G. Orientation of the water dipole

Ordering of the water dipole in the vicinity of the bilayer–water interface is described by calculating the time averaged projection of the water dipole unit vector $\vec{\mu}(z)$ onto the interfacial normal $\vec{n}$,

$$P(z) = \langle \vec{\mu}(z) \cdot \vec{n} \rangle = \langle \cos\theta(z) \rangle , \tag{4}$$

where z is the z-component of the centre-of-mass of the water molecule and vector $\vec{n}$ points away from the bilayer centre along the z-coordinate.

The data for all the studied cases are shown in Fig. 18. For pure bilayers the results are in agreement with previous studies, e. g. (Patra et al., 2003). When either methanol or ethanol is added, the water dipole becomes less oriented, i. e., the addition of alcohol slightly reduces the amount of ordering. For pure bilayers, and for bilayers with added methanol, the minimum remains at the same distance, at about 1.8 nm from the bilayer centre. For added ethanol the minimum shifts to a smaller distance, to about 1.6 nm. This is a reflection of the fact that ethanol leads to a slightly larger area per lipid and thus a thinner bilayer (see Sec. III.A).

H. Electrostatic potential

To obtain the electrostatic potential across the bilayer the average charge density profile was first computed such that the centre of the bilayer was separately aligned to $z = 0$ for each simulation frame. Then, the electrostatic potential was determined by integrating the charge density twice with the initial condition $V(z = 0) = 0$.

The electrostatic potentials for all studied cases are shown in Fig. 19. For pure DPPC the electrostatic potential was determined to be -589 mV in agreement with previous studies (Patra et al., 2003; Tieleman and Berendsen, 1996). For pure POPC we obtain -507 mV.

The addition of alcohol leads only to small changes in the electrostatic potential. This is what is expected from the results presented so far. The only way in which t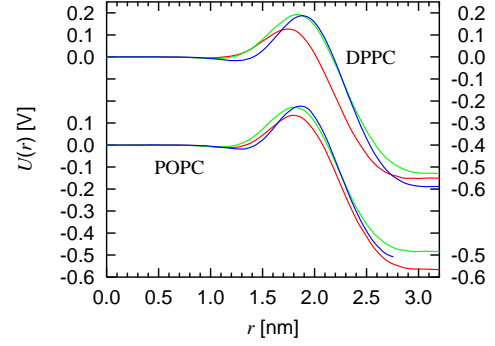he membrane potential could be changed significantly would be by re-arrangement of the $P-N$ angle of the headgroup, resulting in a change of the dipole moment of the lipid headgroup. No such re-arrangement was observed, cf. Fig. 15.

On a superficial level this may seem to be in contradiction to some previous suggestions that the narcotic effects of alcohols are mainly due to a change of the electrostatic potential. We would like to point out, however, that even though the direct effect of alcohol to the potential is small, this does not exclude secondary effects which may lead to a significant change in the electrostatic potential. We return to this issue in Sec. IV.

I. Partitioning coefficients

To measure whether alcohols prefer to stay close to the membrane or rather to be in the water phase, we computed the partitioning coefficients. They provide a thermodynamic quantity characterising a molecule's tendency to choose its environment.

The partitioning coefficient K_{p} is defined as

$$K_{\mathrm{p}} = X_{\mathrm{bilayer}}/X_{\mathrm{water}} , \tag{5}$$

where X_{bilayer} and X_{water} are the moles of solute per kg of solvent (Westh et al., 2001). Equation (5) can be reformulated in terms of the molar concentrations n and the molar masses m as

$$K_{\mathrm{p}} = \frac{(1 - n_{\mathrm{alcohol}}^{\mathrm{water}}) n_{\mathrm{alcohol}}^{\mathrm{bilayer}} m_{\mathrm{water}}}{(1 - n_{\mathrm{alcohol}}^{\mathrm{bilayer}}) n_{\mathrm{alcohol}}^{\mathrm{water}} m_{\mathrm{lipid}}} . \tag{6}$$

Here, $n_{\mathrm{b}}^{\mathrm{a}}$ means the molar concentration of component b in the phase a.

One might be tempted to count the number of alcohol molecules in the lipid phase and in the water phase using some functional definition of where the lipid bilayer interface is located. This approach, however, gives incorrect results as the relevant quantity is not the number of alcohol molecules *inside* the membrane but rather the number of alcohol molecules *influenced* by the membrane.

system	$n_{\text{ethanol}}^{\text{water}}$	$n_{\text{ethanol}}^{\text{lipid}}$	K_{p}
DPPC–ethanol	$(3.98 \pm 0.06) \cdot 10^{-4}$	0.403 ± 0.001	41.6 ± 0.6
POPC–ethanol	$(3.34 \pm 0.04) \cdot 10^{-4}$	0.405 ± 0.001	48.3 ± 0.9
DPPC–methanol	$(4.53 \pm 0.01) \cdot 10^{-3}$	0.278 ± 0.001	2.07 ± 0.02
POPC–methanol	$(4.72 \pm 0.02) \cdot 10^{-3}$	0.272 ± 0.001	1.87 ± 0.02

TABLE IV Results of the partitioning analysis.

Starting point are the mass densities ρ_{water} and ρ_{alcohol} far from the bilayer in the water phase. These are available from Fig. 6, and knowledge of the molar masses gives n_{water}. Multiplying n_{water} by the total number of water molecules in the simulation box gives the number of alcohol molecules that would be there if there was no lipid bilayer. The remaining alcohol molecules thus must be "brought in" by the lipid bilayer.

Our results are summarised in Table IV. Although experimental measurements of partitioning coefficients have been performed (Rowe et al., 1998; Trandum et al., 2000; Westh and Trandum, 1999), we were not able to find experimental data to make exact quantitative comparisons. However, the experimental data for DMPC (Trandum et al., 2000) with ethanol is in qualitative agreement with our results. They are also in agreement with the general trends that K_{p} increases as the lipid tails or the alcohols become longer. As we have studied the system at single temperature we cannot comment on the temperature dependence of the partitioning coefficients.

J. Crossing events

Next, we analyse the penetration of alcohol through the membrane. A quick overview can be obtained by plotting the z-component of the positions of the alcohol molecules. (The positions of all atoms have to be translated for every simulation frame such that the centre of the bilayer does not move). The result is shown in Fig. 20. The density (in space and time) of alcohol molecules is
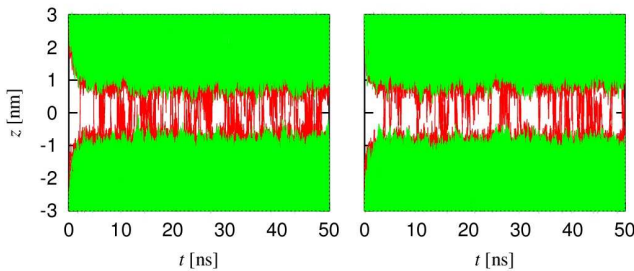

FIG. 20 z-positions of all alcohol molecules as a function of time for DPPC (left) and POPC (right). Ethanol (red) is able to penetrate into the bilayer (located at $z = 0$) much better than methanol (green). Crossing events of ethanol are seen while they are completely absent for methanol.

large in most parts of the diagram such that it is difficult to visually identify individual trajectories.

It is easily seen from Fig. 20 that the density of alcohol molecules is reduced in the centre of the bilayer. In addition, the gap in the centre of the bilayer is smaller for ethanol than it is for methanol. This is in agreement with the mass density profiles presented in Sec. III.B. It is also evident that there is a significant number of events where an ethanol molecule is crossing from one leaflet to the other while no such events are seen for methanol molecules. (Crossing events cannot be inferred from the mass density since these events happen so fast that the resulting mass density of alcohol in the centre of the bilayer is negligible.)

In the simulations, it is directly known which atoms form the lipid molecules of the upper leaflet of the bilayer, and which atoms form the lower leaflet, and which atoms belong to water molecules. The atom nearest to the alcohol molecule then determines in which of the three phases a given alcohol molecule is located at any given moment. In addition, it is also relevant whether an alcohol molecule is hydrogen bonded to some lipid molecule, cf. Sec. III.D.

When all these pieces of information are combined, one arrives at data as shown in Fig. 21 in which we depict a few selected ethanol molecules within a DPPC bilayer. It is seen that, while the alcohol is inside the bilayer, it is hydrogen bonded most of the time. The bonding does not persist for the entire duration of a simulation but there are short breaks in between. This is in agreement with the hydrogen bond lifetime of order 1 ns in Table III while ethanol molecules can stay inside the bilayer much longer than this. Whenever the hydrogen bond is broken, it can either be re-formed shortly afterwards, or the alcohol molecule can try to move to some other place. From the figure it is seen that an alcohol molecule can move to the opposite leaflet of the bilayer but that not all such attempts are successful, i. e., the alcohol molecule may be reflected back.

Using the collected information, each alcohol molecule is at any given moment in one of five different states (water phase, upper leaflet, upper leaflet hydrogen-bonded, lower leaflet and lower leaflet hydrogen-bonded; we will discuss the methanol-containing systems a bit further down). It is of little interest if an alcohol molecule is "scratching" at the surface of the bilayer – rather it is important whether the alcohol molecule reaches the part of the leaflet where it can form a hydrogen bond.

System	successful		unsuccessful	
	number	time [ps]	number	time [ps]
DPPC–ethanol	30	325	123	245
POPC–ethanol	21	375	101	225

TABLE V Number of successful and unsuccessful crossing events, respectively, within 40 ns of trajectory. In addition, the mean time spent in the crossing process is given.
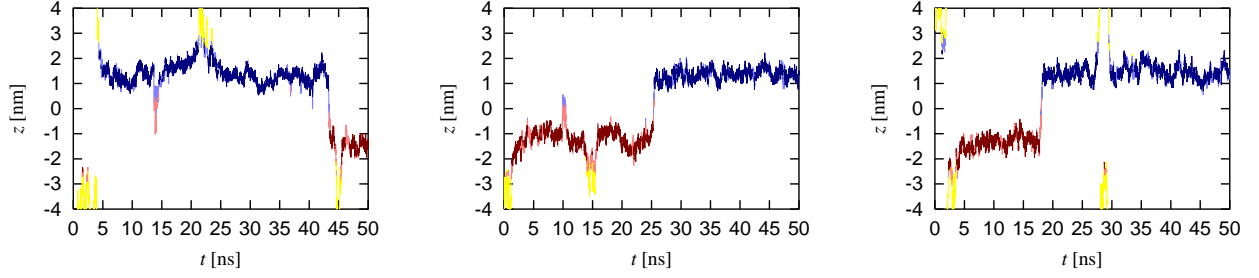
FIG. 21 z-component of the centre-of-mass position of a few tagged ethanol molecule in a DPPC bilayer system. Each figure depicts the trajectory of a different molecule. We have chosen three out of the 90 molecules to give a demonstration of the possible behaviour. The colours red and blue mark in which leaflet of the bilayer the alcohol is located. If the colour is dark red or dark blue, the alcohol is hydrogen bonded to a lipid, otherwise the colour is light red or light blue. If the alcohol is in the water phase, the trajectory is shown in yellow.

This immediately gives functional definitions for different kinetic events that can be used for an automatic analysis. A successful crossing event from the upper to the lower leaflet is for example given by a sequence "upper leaflet hydrogen-bonded → {upper leaflet} → {lower leaflet} → lower leaflet hydrogen-bonded" where the curly braces mean that this step may also be skipped. Similarly, an unsuccessful crossing from top to bottom would be "upper leaflet hydrogen-bonded → {upper leaflet} → lower leaflet → {upper leaflet} → upper leaflet hydrogen-bonded". Other criteria are constructed similarly.

Table V shows the results of the analysis for crossings of ethanol molecules between the two leaflets. A simple calculation shows that ethanol molecules are able to move from one leaflet to the other on a time scale of 130 ns for DPPC and 180 ns for POPC. The number of unsuccessful crossing attempts outnumbers the number of successful attempts by a factor of 4, thereby demonstrating that the hydrophobic tails of the lipid pose a significant barrier to ethanol not only from the outside of the leaflet but also from the inside. For methanol we did not find any crossing events in our simulations, implying that the corresponding time scale must be at least of the order of microseconds.

A closer study of the systems containing methanol is hindered by a problem that is not obvious from any of the data presented so far. As Fig. 22 shows, methanol is virtually never really inside the bilayer, i.e., located such that it no longer has direct contact with the bulk water phase – in all of our data for DPPC and POPC with methanol, we found only a single methanol molecule that had actually lost contact with water.

The above observation is also able to explain why no hydrogen bonds are formed between methanol and the lipids: Water is simply too energetically favourable a binding partner for methanol, or, in other words, the surface tension of water is too high for methanol to leave the water phase. The concept of an alcohol being inside the membrane thus does not apply – topologically, methanols are always located outside the membrane. Rather we need to introduce the concept of a methanol being located in a sufficiently deep well. This can be quantified by counting the number of atoms belonging to lipids within a certain distance around some particular methanol molecule. This number will be much
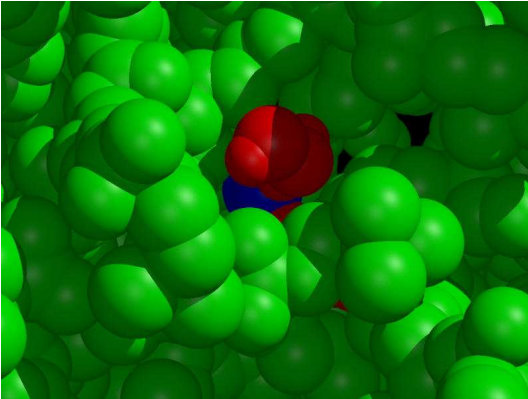

FIG. 22 View from the top onto part of a POPC bilayer with methanol. The lipids are coloured green, methanol is coloured blue and a few selected water molecules are shown in red. It is easily seen than the methanol is located in a cavity together with a few water molecules.
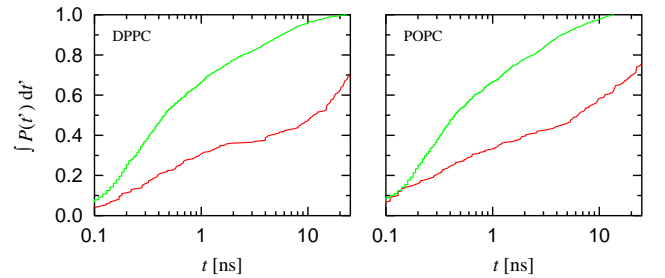

FIG. 23 Distribution $P(t)$ of the time t for which an alcohol molecule stays inside the membrane, left for DPPC, right for POPC. Due to limited statistics, we cannot plot $P(t)$ directly but are limited to the cumulative probability $\int P(t')dt'$.

larger if the methanol is inside such a well. (We use the criterion that the number of atoms belonging to lipid molecules within 0.6 nm is larger than 50.)

Using that functional definition, we are able to treat ethanol and methanol containing systems on a similar footage. While there are no crossing events for methanol, another interesting question still arises, namely the dynamics of alcohol exchange between the membrane and the water phase. Quantitatively, the interesting quantity is the time t between an alcohol molecule entering the membrane and its subsequent leaving it again. Our results are shown in Fig. 23. Since there are only of the order of 200 (1000) events for ethanol (methanol), the statistics is insufficient to compute the probability distribution $P(t)$. Rather, we present the cumulative probability $\int P(t')dt'$, i. e., the probability that an alcohol stays inside the membrane no longer than some time t, since this quantity can be computed without binning the data point. ($P(t)$ follows, in principle, by differentiation of the depicted curves.) It is seen from the figure that the dynamics is much faster for methanol than for ethanol. This comes as no surprise since methanol is not really inside the bilayer – it does not need to cross the bilayer interface but only needs to deform it (to create a well).

IV. DISCUSSION

This study is, to the best of our knowledge, the first detailed computational study characterising the behaviour of lipid bilayers (POPC and DPPC) under the influence of methanol and ethanol. The other existing molecular dynamics study of ethanol and POPC (Feller et al., 2002) concentrated on the comparisons with an NMR study under different conditions (at 10 degrees Celsius close to the gel phase and using an NVT ensemble). To obtain detailed information about alcohol–membrane interactions, it is thus important to study the biologically important fluid phase.

Let us first discuss the area per lipid and bilayer thickness. The increase in the area per lipid is larger for DPPC bilayers (about 7% for ethanol and 6% for methanol) as compared to POPC systems (5% for ethanol and 3% for methanol). This compares well with the recent micropipette studies of Ly et al. (2002) who used SOPC vesicles under slightly different conditions (20 vol.-% ethanol at room temperature). They observed 9% increase in the area per lipid and 8% decrease in the thickness of the bilayer. Here, we obtained a decrease of 7%–10% (ethanol and DPPC) and 1%–4% (ethanol POPC) in thickness depending on the definition used, see Eq. (1).

As a purely structural effect, it is clear that the membrane thus becomes more permeable to small molecules due to its increased area per lipid. The differences between DPPC and POPC are most likely due to the slightly longer $sn-2$ chain of POPC and the double bond in it. In addition to the effects captured by the average area per lipid, steric constraints seem to make the POPC bilayer less susceptible to penetration of small solutes.

Furthermore, in a recent study Chanturiya et al. (1999) proposed that the penetration of alcohols inside the bilayer, and their binding at it, and the resulting decrease in bending rigidity is a feasible pathway for promoting fusion of cells. Although it is not possible to probe this directly by current computer resources, our observations support the possibility of such a mechanism.

It has been suggested that the preferred location of ethanol close to the membrane dehydrates it (Holte and Gawrisch, 1997; Klemm, 1990, 1998). This should show in the water dipole orientation data, Fig. 18. The relatively small changes in it, and in the electrostatic potential across the membrane, suggest that indirect effects, such as receptor blocking, may be more important in producing changes in these quantities.

To characterise thermodynamic properties, we have measured the partitioning coefficients. Our estimates of K_p for the different alcohol-lipid combinations are given in Table IV. Due to the lack of experimental data, no quantitative comparison could be made but qualitatively experiments and simulations are in agreement.

Short-chain alcohols have an amphiphilic character and it has been known for long that addition of each new CH_2 group – adding a CH_2 group on methanol gives ethanol and so on – has a strong effect on the interactions with membranes. This is indicated by the well known Traube's rule (Adamson and Gast, 1997; Traube, 1891) which states that the addition of a new CH_2 group leads to a decrease in surface tension. In other words, short-chain alcohols have a strong effect on membrane properties and the effect depends on both the length of the hydrophobic part of the alcohol and on concentration. This has also been observed in recent experiments (Ly et al., 2002; Ly and Longo, 2004).

Our data for methanol and ethanol supports these conclusions. Methanol does not penetrate through the lipid tail region which is easily understood by the hydrophobic nature of the lipid tails which are repelling methanol as it is more polar than ethanol. As a second effect, methanol rarely reaches the tail region as each methanol molecule moves together with a small cluster of water molecules when it is trying to enter the membrane. This means that, on one hand, methanol is pulled back into the water phase by this, and, on the other hand, not a single small methanol molecule but a significantly larger dressed particle, or a small cluster, would need to penetrate the membrane.

The analysis of crossing events, i. e., how often the molecules travel through the membrane, showed that ethanol is able to penetrate the membrane easily whereas for methanol not a single crossing event was observed. This confirms the interpretation given above. It is difficult to compare these results directly with experiments but the possibility of such crossing events has been proposed on the basis of NMR studies (Holte and Gawrisch, 1997). The results presented here are, to our knowledge,

the first detailed analysis of crossing events. Further experiments would be needed in order to better characterise the situation as the system here is a simple model system and the relevance of these results to biological systems, in particular yeasts, needs to be better studied. The only such a study we were able to find uses NMR and *Z. mobilis* (Schobert et al., 1996) but direct comparison is not possible due to the different experimental setup.

In the introduction we briefly discussed general anaesthesia and membrane–protein interactions induced by the addition of anaesthetics, such as small alcohols. This was observed in a recent experiment (van den Brink-van der Laan et al., 2004) where the potassium channel KcsA was observed to dissociate due to the changes in lateral membrane pressure induced by small alcohols. Here, we have characterised simple membrane–alcohol systems. The detailed characterisation presented here is essential for extensive simulational studies of membrane–protein–anaesthetic systems. From our results it is obvious that the changes in pure membranes are subtle but the effects of those changes to, e.g., embedded proteins may be significant (Cantor, 1997; Eckenhoff, 2001; Koubi et al., 2001; Tang and Xu, 2002; van den Brink-van der Laan et al., 2004). This is also supported by recent experiments using enflurane and DPPC (Hauet et al., 2003). Similar conclusions have been drawn by Tu et al. (1998) for the interaction of halothane with bilayers. As pointed out by Hauet et al., there are various intriguing questions regarding small molecules and anaesthesia. These questions are related to interactions between membranes and small molecules and computer simulations give a direct access to study them.

Acknowledgments

References

Adachi, T., 2000. A new method for determining the phase in the x-ray diffraction structure analysis of phosphatidylcholine / alcohol. *Chem. Phys. Lipids* 17:93–97.

Adamson, A. W. and A. P. Gast, 1997. Physical Chemistry of Surfaces. Wiley-Interscience, New York, 6th edn.

Armen, R. S., O. D. Uitto, and S. E. Feller, 1998. Phospholipid component volumes: Determination and application to bilayer structure calculations. *Biophys. J.* 75:734–744.

Bemporad, D., J. W. Essex, and C. Luttmann, 2004. Permeation of small molecules through a lipid bilayer: A computer simulation study. *J. Phys. Chem. B* 108:4875–4884.

Berendsen, H. J. C., J. P. M. Postma, W. F. van Gunsteren, A. DiNola, and J. R. Haak, 1984. Molecular dynamics with coupling to an external bath. *J. Chem. Phys.* 81:3684–3690.

Berendsen, H. J. C., J. P. M. Postma, W. F. van Gunsteren, and J. Hermans, 1981. Interaction models for water in relation to protein hydration. In B. Pullman, editor, *Intermolecular Forces*, pages 331–342. Reidel, Dordrecht.

Berger, O., O. Edholm, and F. Jahnig, 1997. Molecular dynamics simulations of a fluid bilayer of dipalmitoylphosphatidylcholine at full hydration, constant pressure, and constant temperature. *Biophys. J.* 72:2002–2013.

Bisson, L. F. and D. E. Block, 2002. Ethanol tolerance in *saccharomyces*. In M. Ciani, editor, *Biodiversity and Biotechnology of Wine Yeasts*, pages 85–98. Research Signpost, Kerala.

Cantor, R., 1997. The lateral pressure profile in membranes: A physical mechanism of general anesthesia. *Biophys. J.* 36:2339–2344.

Cantor, R. S., 2003. Receptor desensitization by neurotransmitters in membranes: Are neurotransmitters the endogenous anesthetics? *Biochemistry* 42:11891–11897.

Chanturiya, A., E. Leikina, J. Zimmerberg, and L. V. Chernomordik, 1999. Short-chain alcohols promote an early stage of membrane hemifusion. *Biophys. J.* 77:2035–2045.

Chiu, S. W., E. Jakobsson, S. Subramanian, and H. L. Scott, 1999. Combined Monte Carlo and molecular dynamics simulation of fully hydrated dioleyl and palmitoyl-oleyl phosphatidylcholine lipid bilayers. *Biophys. J.* 77:2462–2469.

Cramer, A. C., S. Vlassides, and D. E. Block, 2002. Kinetic model for nitrogen-limited wine fermentations. *Biotechnol. Bioeng.* 77:49–60.

da Silveira, M. G., E. A. Golovina, F. A. Hoekstra, F. M. Rombouts, and T. Abee, 2003. Membrane fluidity adjustments in ethanol-stressed *oenococcus oeni* cells. *App. Env. Microbiology* 69:5826–5832.

Eckenhoff, R. G., 2001. Promiscuous ligands and attractive cavities. How do the inhaled anesthetics work? *Mol. Interv.* 1:258–268.

Essman, U., L. Perela, M. L. Berkowitz, H. L. T. Darden, and L. G. Pedersen, 1995. A smooth particle mesh Ewald method. *J. Chem. Phys.* 103:8577–8592.

Falck, E., M. Patra, M. Karttunen, M. T. Hyvönen, and I. Vattulainen, 2004. Lessons of slicing membranes: Interplay of packing, free area, and lateral diffusion in phospholipid / cholesterol bilayers. *Biophys. J.* in print.

Feller, S. E., C. A. Brown, D. T. Nizza, and K. Gawrisch, 2002. Nuclear overhauser enhancement spectroscopy cross-relaxation rates and ethanol distribution across membranes. *Biophys. J.* 82:1396–1404.

Gullingsrud, J. and K. Schulten, 2004. Lipid bilayer pressure profiles and mechanosensitive channel gating. *Biophys. J.* 86:3496–3509.

Hauet, N., F. Artzner, F. Boucer, C. Grabielle-Madelmont, I. Cloutier, G. Keller, P. Leiseur, D. Durand, and M. Paternostre, 2003. Interaction between artificial membrane and enflurane, a general volatile anesthetic: DPPC–enflurane interaction. *Biophys. J.* 84:3123–3137.

Hess, B., H. Bekker, H. J. C. Berendsen, and J. G. E. M.

Fraaije, 1997. LINCS: A linear constraint solver for molecular simulations. *J. Comput. Chem.* 18:1463–1472.

Holte, L. L. and K. Gawrisch, 1997. Determining ethanol distribution in phospholipid multilayers with MAS-NOESY spectra. *Biochemistry* 36:4669–4674.

Kessel, A., D. Tieleman, and N. Ben-Tal., 2004. Implicit solvent model estimates of the stability of model structures of the alamethicin channel. *Eur. Biophys. J.* 33:16–28.

Klemm, W. R., 1990. Dehydration. *Alcohol* 7:49–59.

Klemm, W. R., 1998. Biological water and its role in the effects of alcohol. *Alcohol* 15:249–267.

Koubi, L., M. Tarek, S. Bandyopadhyay, M. L. Klein, and D. Scharf, 2001. Membrane structural perturbations caused by anesthetics and nonimmobilizers: A molecular dynamics investigation. *Biophys. J.* 81:3339–3345.

Koubi, L., M. Tarek, M. L. Klein, and D. Scharf, 2000. Distribution of halothane in a dipalmitoylphosphatidylcholine bilayer from molecular dynamics calculations. *Biophys. J.* 78:800–811.

Lee, B. W., R. Faller, A. K. Sum, I. Vattulainen, M. Patra, and M. Karttunen, 2004. Structural effects of small molecules on phospholipid bilayers investigated by molecular simulations. *Fluid Phase Equil.* in print.

Lindahl, E., B. Hess, and D. van der Spoel, 2001. GROMACS 3.0: A package for molecular simulation and trajectory analysis. *J. Molec. Mod.* 7:306–317.

Löbbcke, L. and G. Cevc, 1995. Effects of short-chain alcohols on the phase behavior and interdigitation of phosphatidylcholine bilayer membranes. *Biochim. Biophys. Acta* 1237:59–69.

Ly, H. V., D. E. Block, and M. L. Longo, 2002. Interfacial tension effect on lipid bilayer rigidity, stability, and area / molecule: A micropipet aspiration approach. *Langmuir* 18:8988–8995.

Ly, H. V. and M. L. Longo, 2004. The influence of short-chain alcohols on interfacial tension, mechanical properties, area / molecule, and permeability of fluid lipid bilayers. *submitted to Biophys. J.* .

Mazzeo, A. R., J. Nandi, and R. A. Levine, 1988. Effects of ethanol on parietal cell membrane phospholipids and proton pump function. *Am. J. Physiol.* 254:G57–G64.

Nagle, J. F. and S. Tristram-Nagle, 2000. Structure of lipid bilayers. *Biochim. Biophys. Acta* 1469:159–195.

Nagle, J. F., R. Zhang, S. Tristram-Nagle, W. Sun, H. I. Petrache, and R. M. Suter, 1996. X-ray structure determination of fully hydrated L_α phase dipalmitoylphosphatidylcholine bilayers. *Biophys. J.* 70:1419–1431.

Pabst, G., M. Rappolt, H. Amenitsch, S. Bernstorff, and P. Laggner, 2000a. X-ray kinematography of temperature-jump relaxation probes the elastic properties of fluid bilayers. *Langmuir* 16:8994–9001.

Pabst, G., M. Rappolt, H. Amenitsch, and P. Laggner, 2000b. Structural information from multilamellar liposomes at full hydration: Full q-range fitting with high quality x-ray data. *Phys. Rev. E* 62:4000–4009.

Pasenkiewicz-Gierula, M., T. Róg, J. Grochowski, P. Serda, R. Czarnecki, T. Librowski, and S. Lochyński, 2003. Effects of carane derivative local anesthetic on a phospholipid bilayer studied by molecular dynamics simulation. *Biophys. J.* 85:1428–1258.

Patra, M., M. Karttunen, M. Hyvönen, E. Falck, P. Lindqvist, and I. Vattulainen, 2003. Molecular dynamics simulations of lipid bilayers: Major artifacts due to truncating electrostatic interactions. *Biophys. J.* 84:3636–3645.

Patra, M., M. Karttunen, M. T. Hyvönen, E. Falck, and I. Vattulainen, 2004. Lipid bilayers driven to a wrong lane in molecular dynamics simulations by subtle changes in long-range electrostatic interactions. *J. Phys. Chem. B* 108:4485–4494.

Rowe, E. S., F. Zhang, T. W. Leung, J. S. Parr, and P. T. Guy, 1998. Thermodynamics of membrane partitioning for a series of n-alcohols determined by titration calorimetry: Role of hydrophobic effects. *Biochemistry* 7:2430–2440.

Schobert, S. M., B. E. Chapman, P. W. Kuchel, R. M. Wittig, J. Grotendorst, P. Jansen, and A. A. de Graaf, 1996. Ethanol transport in *Zymomonas mobilis* measured by using in vivo nuclear magnetic resonance spin transfer. *J. Bacteriology* 178:1756–1761.

Tang, P. and Y. Xu, 2002. Large-scale molecular dynamics simulations of general anesthetic effects on the ion channel in the fully hydrated membrane: The implication of molecular mechanisms of general anesthesia. *Proc. Natl. Acad. Sci. USA* 99:16035–16040.

Tieleman, D., M. Sansom, and H. Berendsen, 1999. Alamethicin helices in a bilayer and in solution: Molecular dynamics simulations. *Biophys. J.* 76:40–49.

Tieleman, D. P. and H. J. C. Berendsen, 1996. Molecular dynamics simulations of a fully hydrated dipalmitoylphosphatidylcholine bilayer with different macroscopic boundary conditions and parameters. *J. Chem. Phys.* 105:4871–4880.

Trandum, C., P. Westh, K. Jørgensen, and O. G. Mouritsen, 2000. A thermodynamic study of the effects of cholesterol on the interaction between liposomes and ethanol. *Biophys. J.* 78:2486–2492.

Traube, I., 1891. Ueber die Capillaritätsconstanten organischer Stoffe in wässerigeb Lösungen. *Justus Liebig's Ann. Chem.* 265:27–55.

Tu, K., M. Tarek, M. L. Klein, and D. Scharf, 1998. Effects of anesthetics on the structure of a phospholipid bilayer: Molecular dynamics investigation of halothane in the hydrated liquid crystal phase of dipalmitoylphosphatidylcholine. *Biophys. J.* 75:2123–2134.

van den Brink-van der Laan, E., V. Chupin, J. A. Killian, and B. de Kruijff, 2004. Small alcohols destabilize the KcsA tetramer via their effect on the membrane lateral pressure. *Biochemistry* 43:5937–5942.

Vogel, M., C. Münster, W. Fenzl, and T. Salditt, 2000. Thermal unbinding of highly oriented phospholipid membranes. *Phys. Rev. Lett.* 84:390–393.

Westh, P. and C. Trandum, 1999. Thermodynamics of alcohol–lipid bilayer interactions: Application of a binding model. *Biochim. Biophys. Acta* 1421:261–272.

Westh, P., C. Trandum, and Y. Koga, 2001. Binding of small alcohols to a lipid bilayer membrane: Does the partitioning coefficient express the net affinity? *Biophys. Chem.* 89:53–63.